Compression of Polymer Interphases

Harry J. Ploehn

Department of Chemical Engineering, Texas A&M University, College Station, Texas 77843-3122

Received June 18, 1993; Revised Manuscript Received November 30, 1993•

ABSTRACT: Beginning with fundamental conservation postulates, we construct a generic free energy balance for systems containing polymer interphases undergoing reversible, isothermal deformations. At constant mass, the differential Helmholtz free energy (and the total differential work) equals the total stress times strain in the system. We identify work potentials corresponding to different modes of deformation for a polymer interphase confined between two parallel planar surfaces. For deformations that change the interphase area at constant intersurface separation, the work potential is the surface tension times the differential change in area. However, the work potential for compression of the interphase at constant area is not given by the variation of the surface tension. Instead, it equals the stress (i.e. disjoining pressure) evaluated at the midpoint between the surfaces as required by direct application of conservation of linear momentum. Calculations using continuum-based self-consistent theory show that the work per area for compression of adsorbed polymer layers is considerably more repulsive than the interaction based on the change in surface tension. Without using any arbitrary adjustment of parameters, we find satisfactory quantitative agreement between model predictions and experimental data for the interaction of polystyrene layers adsorbed on mice from cyclopentane at temperatures near the theta point.

I. Introduction

The concept of balancing attractive and repulsive interparticle forces to control colloidal stability has been a paradigm of colloid science ever since the work of Derjaguin and Landau[1] and Verwey and Overbeek.[2] In addition to the van der Waals and electrostatic forces treated in DLVO theory, "steric" or polymeric forces mediated by surfactant or polymer molecules also play an important role in colloidal suspensions found in nature and technology. The continuing interest in understanding polymeric interparticle forces can be attributed to their ubiquity as well as the flexibility and degree of control they bring to colloidal formulations.

Polymer molecules in solution may adsorb onto or be depleted from the surfaces of colloidal particles.[3] Chemical grafting or other forms of tethering are also of interest.[4] In all cases, the spatial distribution of the polymer in the vicinity of the particle–medium interface is inhomogeneous. The region of polymer inhomogeneity is aptly called an "interphase" because its length scale is considerably larger than that of interfaces separating phases composed of small molecules. Changes in the spatial distributions of polymer and solvent are generated when two distinct polymer interphases are brought into proximity. The free energy of the system changes, as well. The interaction energy is the difference between the free energies of the system at finite and infinite separation, and the interaction force is the negative derivative of the free energy with respect to separation. Prediction of polymeric interaction energies and forces thus depend upon a comprehensive understanding of the structure of polymer interphases and their response to deformation.

Before we consider polymeric forces, it is instructive to recall the treatment of electrostatic forces by Verwey and Overbeek.[2] They computed the free energies of a single planar electrostatic double layer and two planar double layers at finite separation. The interaction energy is the difference between the free energies at finite and infinite separation. They show that this derivation, based on the conservation of energy, is entirely equivalent to one based on the conservation of linear momentum, i.e. a force balance. Verwey and Overbeek review three routes which lead to the same result: the force per unit area, or disjoining pressure, acting between charged surfaces equals the difference between the osmotic pressure at the center of the gap and that in the bulk (homogeneous) solution. The stress also equals the negative derivative of the free energy with respect to separation and does not depend explicitly upon the conditions at the surface.

Likewise, for compression of polymer interphases, the conservation of energy and the conservation of linear momentum should produce the same expression for the free energy of interaction or, equivalently, the stress.

Mackor and van der Waals[5] initiated the analysis of polymeric interactions based on the conservation of energy. For interactions of two planar layers of adsorbate at constant temperature, volume, interphase area, and number of moles of each component k (T, V, A_s, and N_k, respectively), the difference in the free energy F between infinite and finite separation is written as

$$F - F^* = 2A_s(\gamma - \gamma^*) + \sum_k N_k(\mu_k - \mu_k^*) \qquad (1)$$

where γ is the surface tension, μ_k is the chemical potential of component k, and the asterisk denotes the infinite separation state. Equation 1 is based on the integral characteristic function

$$F = 2A_s\gamma + \sum_k \mu_k N_k \qquad (2)$$

with the Gibbs and Helmholtz free energies both equivalent to F if the system is incompressible. Using eq 1, Mackor and van der Waals proved that if the adsorbed layers are in equilibrium with an infinite amount of bulk solution, then the free energy difference is exactly

$$F - F^* = 2A_s(\gamma - \gamma^*) \qquad (3)$$

because, in effect, $\mu_k - \mu_k^*$ goes to zero faster than N_k diverges. Thus the disjoining pressure π is found to be

• Abstract published in *Advance ACS Abstracts*, February 1, 1994.

0024-9297/94/2227-1627$04.50/0

$$\pi \equiv -\frac{1}{A_s}\left(\frac{\partial F}{\partial h}\right)_{T,V,A_2,\mu k} = -2\left(\frac{\partial \gamma}{\partial h}\right)_{T,V,A_s,\mu_k} \quad (4)$$

where h is the separation of the planes. Ash et al.[6] obtained eq 4 by postulating the inclusion of a work term $-A_s\sigma\, dh$ in the total differential of the internal energy. They derived a Gibbs–Duhem equation which yields eq 4 when the chemical potentials of all components are held constant.

Subsequent predictions of the interaction energy and stress (disjoining pressure) for the reversible isothermal compression of polymer interphases[3,5-13] are invariably based on eqs 3 and 4. These calculations show that for adsorbed polymer layers in complete equilibrium with bulk solution, the interaction energy decreases with the separation, the stress is negative, and the interaction is monotonically attractive.

By analogy with electrostatic interactions, conservation of linear momentum indicates that the disjoining pressure arising from the interaction of two planar adsorbed polymer layers equals the difference between the osmotic pressure at the center of the gap and that in the bulk solution. Published calculations based on mean-field lattice models,[7,10] mean-field continuum models,[11] and scaling theory[8] show that for polymer adsorbed or grafted on surfaces in Theta or good solvents, the osmotic pressure at the center of the gap is greater than that in bulk solution, and the difference increases as the layers are compressed. These results imply that the stress is positive and the interaction is monotonically repulsive. Thus the conservation of energy and the conservation of linear momentum lead to contradictory predictions for the sign of polymeric interactions.

The purpose of the following analysis is to resolve this contradiction through careful construction of energy and linear momentum balances for processes that produce deformation of polymer interphases. Beginning with rigorous expressions for the conservation of total mass, mass of individual components, linear and angular momentum, total energy, and the entropy inequality, we derive a free energy balance that shows that the differential change of Helmholtz free energy equals stress times strain integrated over the volume of the system. For deformations that change the area of an interphase at constant intersurface separation, we recover the surface tension from the variation of the free energy with interfacial area. For deformations that compress an interphase at constant area, we recover an expression for the interaction stress as the variation of the free energy with intersurface separation.

We then review an implementation of continuum-based self-consistent mean-field theory for adsorption of homopolymer on two proximate planar surfaces.[22] We develop predictions for the work per area for compression of interphases in complete equilibrium with bulk solution, as well as interphases in which the amount of adsorbed polymer is held constant. The predictions of the model are compared with experimental results for interaction of adsorbed polystyrene layers in cyclopentane obtained from measurements utilizing the surface forces apparatus.

II. Conservation Principles for Interphase Compression

A. Interphase Models. An interphase is a three-dimensional region in which material properties vary continuously as one passes from one bulk (homogeneous) phase into another. When the length scale associated with the thickness of the interphase is much less than any other length scale in a given situation, the analysis of the properties of an interphase is facilitated by assigning its properties to a Gibbs dividing surface. This "macroscale" point of view is used by Slattery[14] and Edwards et al.[15] in their treatments of the mechanics of continua which contain interphases. Three-dimensional "microscale" models have greater utility when the interphase length scale becomes comparable to an experimental length scale. Such a situation occurs when surfaces bearing polymer molecules are compressed to separations on the order of the polymer's radius of gyration. Edwards et al.[15] have developed a rigorous treatment of the continuum mechanics of three-dimensional interphases which is consistent with two-dimensional models in the appropriate limits.

Here, we consider interphases created by the interaction of a polymer solution with the surface of a solid. We treat the solid–fluid interface as a two-dimensional surface which acts as part of the boundary of our system. The system contains homogeneous bulk solution and a polymer interphase. We will view the interphase as a three-dimensional domain, in which the material properties are inhomogeneous but continuous, which merges continuously into the bulk solution. Thus we shall use forms of the fundamental conservation postulates as specified for single phase systems.

B. Generic Free Energy Balance. Our goal is a generic expression for the variation of the free energy of the system caused by an arbitrary deformation. This problem is commonly encountered in solid mechanics,[16] but multicomponent materials are usually treated in the context of fluid mechanics[14] wherein rates of deformation are of primary interest. Hence it is convenient to express the necessary conservation principles in rate form; generalization to a variational expression will be made after the details of a particular mode of deformation are introduced in the next section.

Consider a multicomponent polymer solution containing N_k moles of component k at temperature T. We assume that the partial molar volume $\bar{V}_k$ of each component is constant, implying that the solution is incompressible. Let $\rho^m(\vec{r})$ be the local mass density of the mixture. The conservation of mass at every point requires

$$\frac{d_v\rho^m}{dt} + \rho^m \nabla\cdot\vec{v} = 0 \quad (5)$$

where $\vec{v}$ is the mass-average velocity and

$$\frac{d_v(\,)}{dt} \equiv \frac{\partial(\,)}{\partial t} + \vec{v}\cdot\nabla(\,) \quad (6)$$

denotes the time derivative following the mass-average motion of a material particle. Since the solution is incompressible, we must have

$$\rho^m \nabla\cdot\vec{v} = 0 = \frac{d_v\rho^m}{dt} \quad (7)$$

so that an observer moving (and deforming) with a differential piece of the mixture would observe no change in the average mass density with time. For a stationary observer, the rate of mass accumulation equals the net rate of mass input at a point (that is, per unit volume).

Neglecting body forces, chemical reactions, and radiant energy transmission, the conservation of total energy at every point and eq 7 require

$$\frac{d_v}{dt}\left[\check{U} + \frac{1}{2}\rho^m v^2\right] = \nabla\cdot(\mathbf{T}\cdot\check{v}) - \nabla\cdot\check{q} \quad (8)$$

where $\check{U}$ is the internal energy per unit volume, T is the stress tensor, and $\check{q}$ is the total energy flux vector. Conservation of angular momentum necessitates the symmetry of the stress tensor. The scalar product of the velocity with the differential equation for the conservation of linear momentum produces

$$\frac{d_v}{dt}\left[\frac{1}{2}\rho^m v^2\right] = \nabla\cdot(\mathbf{T}\cdot\check{v}) - \mathrm{tr}(\mathbf{T}\cdot\mathbf{D}) \quad (9)$$

which can be substracted from eq 8 to give the differential internal energy balance

$$\frac{d_v\check{U}}{dt} = \mathrm{tr}(\mathbf{T}\cdot\mathbf{D}) - \nabla\cdot\check{q} \quad (10)$$

in which **D** is the rate of deformation tensor and "tr" denotes the trace of a tensor.

For processes that change the state of the system slowly and reversibly, the entropy inequality (second law of thermodynamics) becomes an equality

$$T\frac{d_v\check{S}}{dt} + T\nabla\cdot\left(\frac{\check{e}}{T}\right) = 0 \quad (11)$$

in which $\check{S}$ is the entropy per unit volume and $\check{e}$ is the thermal energy flux vector. Subtraction of eq 11 from 10 and introduction of the Helmholtz free energy per unit volume $\check{A} \equiv \check{U} - T\check{S}$ yields

$$\frac{d_v\check{A}}{dt} = -\check{S}\frac{d_vT}{dt} + \mathrm{tr}(\mathbf{T}\cdot\mathbf{D}) - \nabla\cdot(\check{q} - \check{e}) - \frac{1}{T}\check{e}\cdot\nabla T \quad (12)$$

The entropy inequality places other constraints upon material behavior. In particular, it can be proven[14] that the difference between $\check{q}$ and $\check{e}$ equals the flux of free energy carried by mass

$$\check{q} - \check{e} = \sum_k \mu_k\check{J}_k \quad (13)$$

where $\check{J}_k$ is the molar flux (moles per area per time) of component k with respect to the mass-average motion of a material particle. The chemical potential used here is a generalized potential which includes contributions arising from spatial inhomogeneity as well as the constraints of incompressibility and "tethering" of polymer in the interphase on the time scale of experiments.

We now assume that at equilibrium, the chemical potential of each component equals its value in bulk solution, μ_k^b, which is constant. The mass balance for each component k is given by

$$\nabla\cdot\check{J}_k = \frac{d_v\rho_k}{dt} \quad (14)$$

in the absence of chemical reactions. Substitution of eqs 13 and 14 into eq 12 and constant μ_k^b and T produce

$$\frac{d_v\check{A}}{dt} = \mathrm{tr}(\mathbf{T}\cdot\mathbf{D}) + \sum_k \mu_k^b\frac{d_v\rho_k}{dt} \quad (15)$$

valid at every point in the system.

The transport theorem[14]

$$\frac{d}{dt}\int_V Q\,dV = \int_V\left(\frac{d_vQ}{dt} + Q\nabla\cdot\check{v}\right)dV = \int_V\frac{d_vQ}{dt}dV \quad (16)$$

indicates how the order of time derivatives and volume integration can be interchanged for any scalar, vector, or tensor-valued quantity Q. The second equality in eq 16 applies to incompressible systems for which $\nabla\cdot\check{v} = 0$. Utilizing eq 16, integration of eq 15 over the volume of the system gives

$$\frac{dA}{dt} = \int_V \mathrm{tr}(\mathbf{T}\cdot\mathbf{D})\,dV + \sum_k \mu_k^b\frac{dN_k}{dt} \quad (17)$$

as the desired accounting statement for the Helmholtz free energy A for reversible deformations at constant temperature.

We can now convert the free energy balance, eq 17, from the rate form to a variational equation. First, we recognize[17] that **D** equals the time derivative of the (right) stretch tensor **U**. Time derivatives may be generalized to differential variations through the chain rule, $\delta() = (d()/dt)\delta t$. The variational form of eq 17 is thus

$$\delta A = \int_V \mathrm{tr}(\mathbf{T}\cdot\delta\mathbf{U})\,dV + \sum_k \mu_k^b\delta N_k \quad (18)$$

indicating that the differential accumulation of A in the system equals the amount of mechanical energy converted into internal energy by differential deformation at each point throughout the system, plus the amount of free energy input due to differential addition of matter to the system.

C. Compression of a Planar Interphase. We now consider an interphase which occupies a region between two parallel planar surfaces, each of area A_s, separated by a distance $2z_m$. The coordinate direction normal to the surfaces is z with the origin at one of the surfaces. The midpoint between the surfaces is at $z = z_m$. We will restrict our attention to compression of the interphase by an external stress acting in the direction normal to the planar surfaces. The first objective is to calculate (via eq 18) the free energy variation associated with the deformation that results from the action of this external stress.

We envision that the compression of the interphase proceeds through a sequence of states that are in hydrostatic equilibrium. During a differential amount of compression, shear stresses and transverse (lateral) chemical potential gradients will develop. Before the next episode of differential compression, the distribution of components is allowed to rearrange to eliminate the transverse chemical potential gradients. This allows us to simplify the stress tensor according the conditions of hydrostatic equilibrium as outlined by Davis and Scriven.[38]

The stress tensor can be written as the sum of an isotropic solvent pressure P_0 and an anisotropic osmotic stress **S** via[39]

$$\mathbf{T} \equiv -P_0\mathbf{I} + \mathbf{S} \quad (19)$$

The solvent pressure is the part of the total pressure that is constant among all phases that have equal solvent chemical potential,[39] thus we choose

$$P_0 = P^b - \Pi^b \quad (20)$$

where Π^b is the osmotic pressure of bulk solution.

Under conditions of hydrostatic equilibrium,[38] the osmotic stress in a planar interphase near a structureless

surface has the form[39]

$$\mathbf{S} = S_T(\mathbf{I} - \tilde{\mathbf{e}}_z\tilde{\mathbf{e}}_z) + S_N\tilde{\mathbf{e}}_z\tilde{\mathbf{e}}_z \quad (21)$$

where S_T and S_N are the principal stresses in the transverse and normal directions. In bulk solution, $\mathbf{T}$ is isotropic and equal to $-P^b\mathbf{I}$. Equations 19–21 show that $S_T = S_N = -\Pi^b$ in bulk solution. In general, S_T is a function of z, but hydrostatic equilibrium requires that $S_N = -\Pi^b$ everywhere in the interphase.[38] Thus the stress tensor becomes

$$\mathbf{T} = -P^b\mathbf{I} + (S_T + \Pi^b)(\mathbf{I} - \tilde{\mathbf{e}}_z\tilde{\mathbf{e}}_z) \quad (22)$$

In the next section, we will choose the form of S_T to make the energy balance consistent with established thermodynamic expressions for inhomogeneous polymer interphases.[7-13,19-23,38]

The right stretch tensor $\delta\mathbf{U}$ is real and symmetric; thus it possesses three principal directions with real values.[17] The diagnoal elements δU_{ii} ($i = x, y, z$) equal the stretches in the principal directions and are defined by the kinematics of the compression. Consider a line segment which is oriented in one of the principal directions and which has unit length when the surfaces are separated by a finite but large distance. As the interphase is compressed, the line segment deforms with the material points of the continuum. The dilation λ_i is the length of the line segment in the deformed state. The values of δU_{ii} are given in terms of dilations by[17,18]

$$\delta U_{ii} = \delta\lambda_i/\lambda_i \quad (23)$$

which are positive for extension and negative for compression.

With $\mathbf{T}$ and $\delta\mathbf{U}$ specified by eqs 22 and 23, we can evaluate the integral term in eq 18 after dividing the domain V into bulk (V^b) and interphase (V^i) contributions. However, the procedure is not straightforward because the integration domain depends on the deformation.[21] We circumvent this difficulty by introducing a change of variables that transforms the domain of integration into that of a reference configuration,[17,18] e.g. the state in which the planes are separated by a finite but large distance. After some manipulation,[21] we find

$$\delta A = -P^b\delta V + \sum_k \mu_k{}^b\delta N_k + \delta\int_{V^i}(S_T + \Pi^b)\,dV + \int_{V^i}\left\{\frac{\delta[(S_T + \Pi^b)\lambda_z]}{\lambda_z}\right\}dV \quad (24)$$

where $\lambda_A \equiv \lambda_x\lambda_y$. For systems consisting a single homogeneous phase ($V^i = 0$), eq 24 reduces to the fundamental thermodynamic equation defining variations of A at constant temperature.

D. Surface Tension, Disjoining Pressure, and Work. For an interphase occupying the region between parallel planes, $V^i = 2A_s z_m$ and $dV^i = 2A_s dz_m$, assuming that the local properties in the interphase do not vary in directions parallel to the surfaces. The surface tension[25]

$$\left(\frac{\delta A}{\delta[2A_s]}\right)_{T,V,N_N,z_m} \equiv \gamma \quad (25)$$

can be evaluated from eq 24 with the limits of the integrals ranging from 0 to z_m. The result[21]

$$\gamma = \int_0^{z_m}[S_T + \Pi^b]\,dz = \int_0^{z_m}[\Pi^b - \Pi(z)]\,dz \quad (26)$$

is consistent with the Kirkwood–Buff form[15,23] for three-dimensional interphases if we choose $S_T \equiv -\Pi(z)$ where $\Pi(z)$ is the local osmotic pressure in the interphase.

The external stress which causes the compression, π, also known as the disjoining pressure, is related to the Helmholtz free energy by[24,25]

$$\frac{1}{2A_s}\left(\frac{\delta A}{\delta z_m}\right)_{T,V,N_k,A_s} = -\pi \quad (27)$$

so that π is positive for repulsive interactions which increase the free energy of the system. The disjoining pressure can therefore be calculated from the appropriate work potential (i.e. Helmholtz free energy variation) for compression of the interphase. This work potential is the product of stress and strain integrated over the domain of the interphase as shown in the previous section.

Evaluation of the disjoining pressure utilizing eqs 24 and 27 produces[21]

$$\pi = -(S_T{}^m + \Pi^b) = \Pi^m - \Pi^b \quad (28)$$

where the superscript m denotes evaluation of the function at $z = z_m$. The disjoining pressure thus equals the difference between the osmotic pressure at the center of the gap and that in the bulk (homogeneous) solution. Furthermore, π does not depend explicitly upon the conditions at the surfaces. Identical results for the form of π can be developed from conservation of linear momentum through an analogy with electrostatic interactions,[2] from the integral mechanical energy balance,[21] or from a free energy balance as shown above. All analyses show that for full equilibrium conditions, π equals the difference between the osmotic pressures at the midpoint of the interphase ($z = z_m$) and in bulk solution.

When the exchange of some components between the interphase and bulk is constrained, an additional "deviatoric" contribution appears in the osmotic stress.[21] This case is considered in the next section.

For reversible processes at constant temperature, the change in the Helmholtz free energy is the total work performed by the surroundings on the system. The change in A per unit area of interphase can be found from eq 28 as the integral of π from infinite to finite separation[24,25]

$$\frac{W}{2A_s} = \frac{\Delta A}{2A_s} = -\int_\infty^{z_m}\pi(u)\,du \quad (29)$$

while holding T, V, N_k, and A_S constant.

III. Self-Consistent Field Theory

A. Continuum Field Equations for Polymer Adsorption. In the previous section, we used fundamental conservation principles to develop a free energy balance which yields the correct work potential for compression of a polymeric interphase. In order to calculate the disjoining pressure and work per area for compression, we utilize self-consistent field (SCF) theory to model structure within polymeric interphases. We consider the particular situation of polymer adsorption on two opposing, parallel, planar surfaces. The governing equations of our SCF model for the structure of adsorbed polymer layers have already been developed in detail.[22] Therefore we will only give a minimal description here.

The statistical mechanical foundation for the continuum-based SCF model of inhomogeneous polymeric interphases was established by Helfand[19] and was completed by Hong and Noolandi.[20] The analogous lattice-

based SCF model was developed by Scheutjens and Fleer.[7,10] The SCF model used here is built entirely upon this foundation as discussed previously.[22]

SCF theory began with Edward's analogy[26] between the contour of a polymer molecule and the random trajectory of a particle diffusing in an external potential field. Mathematically, the random walk is embodied in a function $q(z,t)$ which is the probability density for a chain of t polymer segments beginning anywhere and ending at a distance z from one of the surfaces. Helfand[19] showed that q satisfies a modified diffusion equation. Appropriate initial and boundary conditions for adsorption in the gap between two surfaces reflect the equal likelihood of chains beginning anywhere, the energy reduction per polymer segment adsorbed, and the symmetry of the geometry about the gap midpoint at $z = z_m$.

The random walk of the polymer contour is biased by a potential energy field arising from polymer–polymer and polymer–solvent interactions. Since the field is determined by polymer configurations governed by a diffusion equation which, in turn, depends on the field, it has "self-consistent" character. An explicit relationship between the self-consistent field, w_p, and the local polymer density, ρ_p (moles of monomers per volume), results from functional minimization of the free energy with respect to variations in ρ_p. Our previous heuristic development[22] is consistent with the formal statistical mechanical analysis.[20] The result

$$\mu_p - \left[w_p + \frac{RT}{Z_p}\ln(\tilde{V}_p\rho_p)\right] + g + \tilde{V}_p(\Pi - \Pi^b) = \mu_p{}^b \quad (30)$$

is an equilibrium condition that identifies w_p as an additional potential energy that maintains the inhomogeneity of the adsorbed polymer layer. The field is modified by a term that corrects for the nonlocal translational entropy of polymer configurations; RT is the thermal energy per mole, Z_p is the number of polymer segments per chain, and $\tilde{V}_k\rho_k \equiv \varphi_k$ is the volume fraction of component k. The Lagrange multiplier g is nonzero when the exchange of polymer between the interphase and bulk solution is hindered by diffusive or convective limitations. Lastly, the osmotic pressure difference $\Pi - \Pi^b$ maintains incompressibility through variations in the local composition. Equation 30 is an example of generalized "membrane" equilibrium as discussed by Lyklema.[25]

Once the statement of equilibrium given by eq 30 has been identified, the Helmholtz free energy of the system can be shown[22] to have the standard form

$$A = -P^bV + \sum_k \mu_k{}^b N_k + A_s\gamma \quad (31)$$

with the surface tension given by

$$\gamma = \int_0^{z_m}(\Pi^b - \Pi - g\rho_p)\,dz \quad (32)$$

When the polymer may move freely between the interphase and bulk solution, $g \equiv 0$ as necessitated by comparison with eq 26. When the exchange of polymer is constrained, we select $S_T \equiv -(\Pi + 2g\rho_p)$ so that eqs 26 and 32 are consistent. The disjoining pressure in this case is given by

$$\pi = -(S_T{}^m + \Pi^b) = \Pi^m - \Pi^b + 2g(z_m)\rho_p{}^m \quad (33)$$

The general forms of the self-consistent field equations, given in the previous publication,[22] are made dimensionless by scaling distance from one of the surfaces (z), segment rank (t), and energy with the polymer segment length l, Z_p, and RT, respectively. A semianalytical solution may be obtained by expanding $q(z,t)$ in powers of $1/Z_p$. However, we retain the form of w_p given in eq 30: normalization and equilibrium conditions demand that w_p depend on Z_p in bulk solution. Thus we neglect chain "end effects" upon adsorbed layer structure. The lowest order problem in powers of $1/Z_p$ is

$$0 = \frac{1}{6}\frac{d^2q_0}{dz^2} - w_pq_0 \quad (34a)$$

$$\frac{dq_0}{dz}(z_m) = 0 \quad (34b)$$

$$\frac{d\ln q_0}{dz}(0) = -\chi_s \quad (34c)$$

$$q_0{}^2 = \tilde{V}_p\rho_p = \varphi_p \quad (34d)$$

where the boundary conditions reflect the symmetry at the midplane (eq 34b) and the free energy reduction [26] χ_s per polymer segment adsorbed in place of a solvent molecule at the surface $z = 0$ (eq 34c). Equation 34d is used to change variables from q_0 to polymer volume fraction φ_p during the integration of eq 34a.

The integration of eq 34a has been discussed before.[22] The first integral is

$$\left(\frac{d\varphi_p}{dz}\right)^2 = 24\varphi_p[F(\varphi_p,g) - F(\varphi_p{}^m,g)] \quad (35)$$

with the boundary condition 34c defining

$$F(\varphi_p,g_p) \equiv \tilde{V}_p\Delta a + g\varphi_p + \frac{1}{Z_p}[-\varphi_p\ln(\varphi_p) + \delta_p{}^b\ln(\varphi_p{}^b) + \varphi_p - \varphi_p{}^b] \quad (36)$$

where

$$\Delta a \equiv a_h - (\rho_p\mu_p{}^b + \rho_s\mu_s{}^b - P^b) \quad (37)$$

is a mixing free energy density. The forms of a_h and μ_k appropriate for the extended form of the Flory–Huggins equation of state used here are given in the Appendix. An equation analogous to eq 36 exists for $F(\varphi_p{}^m, g)$ with $\varphi_p{}^m \equiv \varphi_p(z_m)$ treated as a parameter. The second integral of eq 34a

$$z = -\int_{\varphi_0}^{\varphi_p}\frac{du}{\{24u[F(u,g) - F(\varphi_p{}^m,g)]\}^{1/2}} \quad (38)$$

gives the polymer volume fraction as an implicit function of the distance from the surface and the surface volume fraction $\varphi_0 \equiv \varphi_p(0)$.

The solution is completely determined by three unknowns, φ_0, $\varphi_p{}^m$, and g which depend implicitly upon z_m. These unknowns are found from the simultaneous solution of three equations

$$\varphi_0\chi_s{}^2 - 6F(\varphi_0,g) = 0 \quad (39)$$

$$\int_{\varphi_0}^{\varphi_p{}^m}\frac{du}{\{24u[F(u,g) - F(\varphi_p{}^m,g)]\}^{1/2}} + z_m = 0 \quad (40)$$

and

$$\int_{\varphi_0}^{\varphi_p^m} \frac{(u - \varphi_p^b)\,du}{\{24u[F(u,g) - F(\varphi_p^m,g)]\}^{1/2}} + \varphi_{ads} = 0 \qquad (41)$$

which arise from the surface boundary condition 34c, the definition of φ_p^m, and the definition of the dimensionless polymer adsorbed amount φ_{ads}.

For two interacting adsorbed layers under full equilibrium conditions, eqs 39 and 40 are solved iteratively for a given value of z_m. When the exchange of polymer between the interphase and bulk solution is constrained, we fix φ_{ads} from the single surface equilibrium case[22] and then solve eqs 39–41 iteratively as a function of z_m.

B. Parameterization. The present SCF model has no adjustable parameters. All of the physical and chemical characteristics of the polymer, solvent, and adsorbing surface are embodied in eight parameters: $T, l, Z_p, \bar{V}_p, \bar{V}_s, \varphi_k^b, \chi$, and χ_s. The values of T and φ_k^b are given experimental parameters; $\bar{V}_p$ and $\bar{V}_s$ are fixed by the physical properties of the pure components; l, Z_p, and χ are determined through independent experiments involving polymer solutions; and χ_s may be found from displacement experiments involving the polymer, solvent, and surface of interest.[27] Experimental data for fixing model parameters are available for some polymer–solvent systems,[28] although χ_s data are scarce.[27] Fortunately, the predictions of the present SCF model[22] and the Scheutjens–Fleer lattice model[7,10] are not sensitive to the value of χ_s as long as the total segment–surface adsorption energy per polymer molecule is much greater than kT. We have used arbitrary values of χ_s between 1.0 and 1.5, but the predictions are essentially independent of χ_s over this range.[22]

The details of parameter estimation have been discussed at length in the previous publication.[22] The essential point is that we require real polymer molecules and idealized chains of segments to have identical backbone contour lengths and radii of gyration in solution, thus fixing l and Z_p in terms of the average backbone bond length, polymer molecule weight, molecular weight per monomer, and solution radius of gyration or characteristic ratio. Consequently, polymer segments and solvent molecules have different volumes. Molecular volume differences are incorporated in the form of the Flory–Huggins equation of state used here (see Appendix). Hence $\bar{V}_p$ and $\bar{V}_s$ appear as parameters and the appropriate value of χ must be determined from original data for polymer solution phase behavior. The effects of molecular volume differences on the structure of single adsorbed polymer layers are detailed elsewhere.[22]

IV. Results and Discussion

A. Full Equilibrium Interactions. The interphase and the bulk solution are said to be in "full" equilibrium when all components are free to move between regions as the interphase is deformed. The characteristics of compression of two adsorbed polymer layers under full equilibrium conditions are illustrated in Figures 1 and 2 for a typical set of model parameters. Figure 1 shows that as the interphase is compressed, the volume fraction of polymer at the surface remains nearly constant, but the polymer volume fraction at the gap midpoint increases considerably. The compression stress or disjoining pressure, given by eq 28, is therefore monotonically repulsive.

In contrast, de Gennes[8] found that the disjoining pressure for interphase compression was monotonically attractive under full equilibrium conditions. However, de Gennes' analysis is based on the assumption that γA_s

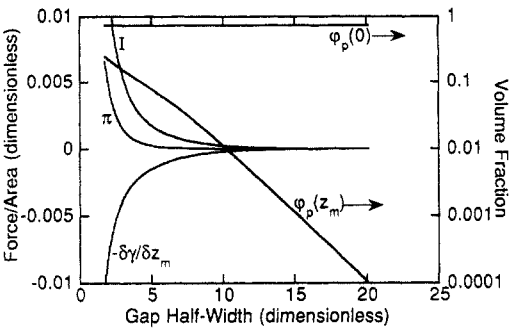

Figure 1. Computed surface volume fraction of polymer $\varphi_p(0)$, midpoint volume fraction of polymer $\varphi_p(z_m)$, and contributions to the disjoining pressure π as functions of the half-width z_m of the gap separating two adsorbing surfaces. The curves labeled $-\delta\gamma/\delta z_m$ and I are contributions to π described by eq 42. Parameters for the full equilibrium calculation include $\chi_s = 1.0$, $\chi = 0.50$, $Z_p = 1000$, $\varphi_p^b = 1.0 \times 10^{-4}$, and $\bar{V}_p = \bar{V}_s$.

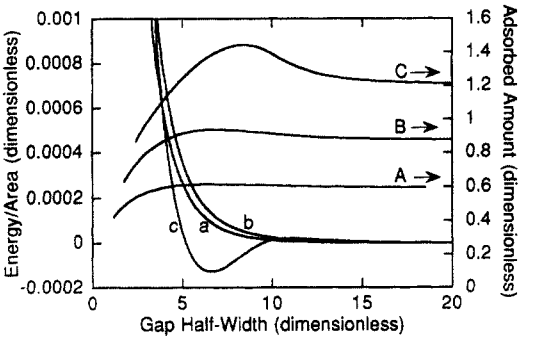

Figure 2. Calculated adsorbed amount of polymer φ_{ads} (curves A, B, and C) and compression work per area $W/2A_s$ (curves a, b, and c) as functions of the half-width z_m of the gap separating two adsorbing surfaces. Curves A + a, B + b, and C + c are for χ = 0.40, 0.50, and 0.55, respectively. Other parameters for the full equilibrium calculation are as in Figure 1.

is the appropriate work potential for interphase compression. In fact, the proper work potential for this case includes an additional term involving the osmotic stress, much like a "$V\delta P$" correction to the Gibbs potential $\delta(PV)$.[21]

The various contributions to the disjoining pressure can be identified by differentiating the surface tension, eq 26, with respect to the gap half-width z_m, producing

$$\pi = -\frac{\delta\gamma}{\delta z_m} - \int_0^{z_m} \frac{\delta\Pi}{\delta z_m}\,dz \qquad (42)$$

The surface tension variation and the negative of the integral term (labeled as "I" in Figure 1) give attractive and repulsive contributions to the disjoining pressure, with the repulsive term dominating at all separations. By analogy with electrostatic interactions, the first term can be rationalized as a "chemical" contribution which becomes more negative as separation decreases and polymer bridging increases. The second term represents osmotic repulsion associated with entropically unfavorable demixing in the gap under these conditions. In the same vein, Evans and Needham[21] characterized the second term as virtual "$V\delta P$" work necessary to maintain incompressibility at all points.

Osmotic effects are more clearly seen in the effect of χ upon compression work and adsorbed amount of polymer as shown in Figure 2. As expected, φ_{ads} is greatest for adsorption from a poor solvent (χ = 0.55, curve C) and least for adsorption from a good solvent (χ = 0.40, curve A) under all conditions. For good and Theta solvents (χ = 0.50, curve B), compression of the interphase leads to a very slight increase of polymer adsorption at intermediate

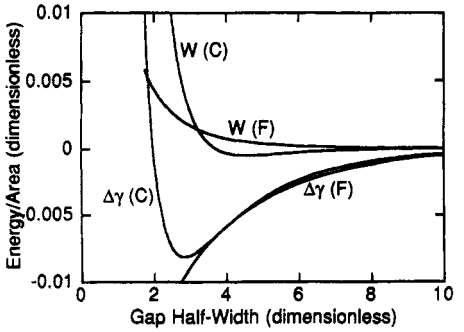

Figure 3. Calculated compression work per area $W/2A_s$ (curves labeled W) and change in surface tension per area $\Delta\gamma$ as functions of the half-width z_m of the gap separating two adsorbing surfaces, for complementary full (F) and constrained (C) equilibrium cases. The parameters are as in Figure 1.

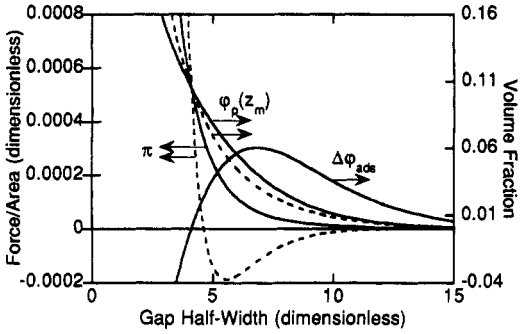

Figure 4. Computed change in polymer adsorbed amount $\Delta\varphi_{ads}$ (full equilibrium), midpoint polymer volume fraction $\varphi_p(z_m)$, and disjoining pressure π as functions of the half-width z_m of the gap separating two adsorbing surfaces. Solid curves are for full equilibrium, and dashed curves are for constrained equilibrium. The parameters are as in Figure 1.

separations and ejection of polymer from the gap at smaller separations. The work of compression (curves a and b) is monotonically repulsive in both cases. For the poor solvent case, polymer adsorption increases considerably at intermediate separations before eventual ejection at smaller separations. The work of compression for this case (curve c) has an attractive minimum. Scheutjens and Fleer[10] and Klein and Pincus[9] reported similar results which were attributed to portions of the polymer interphase having compositions in the unstable sector of the bulk solution phase diagram.

B. Constrained Equilibrium Interactions. In most experiments, the time scale for desorption of polymer molecules from an adsorbing surface is much greater than the characteristic time for deformation of the interphase. Theoretical models[7-13,22] generally handle this situation by assuming that the adsorbed amount of polymer remains constant during the deformation. By minimizing the total free energy of the system subject to this constraint, the models implicitly assume an equilibrium distribution of polymer configurations within the polymer interphase. This situation is therefore characterized as "restricted" or "constrained" equilibrium. The model predictions shown in Figures 3–9 are constrained equilibrium calculations.

Scheutjens and Fleer[10] originally demonstrated that the surface excess Helmholtz free energy (or surface tension) of an interphase in constrained equilibrium must always be greater than or equal to that of an interphase in full equilibrium with bulk solution. Figure 3 shows that the surface tensions predicted by the present model satisfy this requirement. The surface tensions for the full and constrained equilibrium cases are equal when the corresponding interphases have the same adsorbed amount of polymer. However, the work of compression, which equals

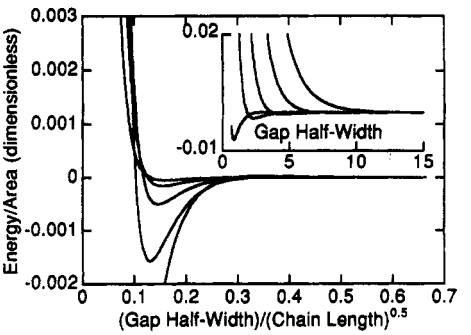

Figure 5. Computed compression work per area ΔA for several polymer chain lengths as functions of the half-width z_m of the gap scaled on $Z_p^{1/2}$. Unscaled interaction curves are shown in the inset. Values of Z_p = 100, 316, 1000, 3160, and 10 000 correspond curves with decreasing depths of attractive minima and increasing repulsion. Other parameters are as in Figure 1.

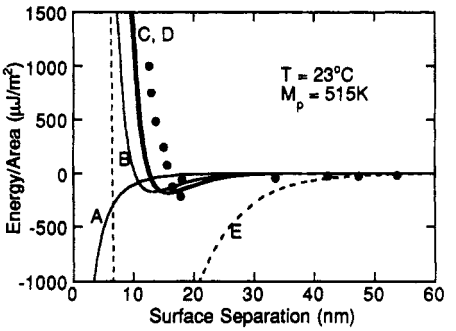

Figure 6. Experimental and calculated compression work per area for two interacting layers of PS (5.15×10^5 g/mol) adsorbed onto mica from CP at 23 °C. The circles are experimental data from ref 30. Curves A–D are the calculated compression work for χ_s = 0.25, 0.50, 1.0, and 1.5, respectively. Curve E is the change in surface tension per area for χ_s = 1.0. Other parameters include χ = 0.484, Z_p = 895, $\varphi_p^b = 1.43 \times 10^{-3}$, $\bar{V}_p$ = 99.1 cm³/mol, and $\bar{V}_s$ = 94.0 cm³/mol.

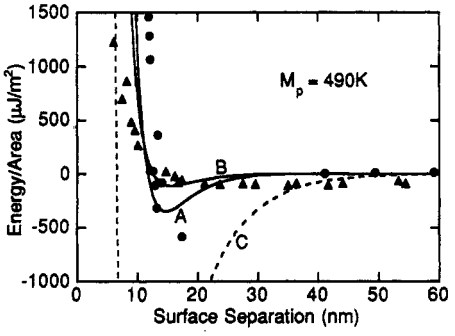

Figure 7. Experimental and calculated compression work per area for two interacting layers of PS (4.90×10^5 g/mol) adsorbed onto mica from CP. The experimental data (ref 30) are for 18 °C (circles, χ = 0.508) and 28 °C (triangles, χ = 0.460). Curves A and B are the corresponding model predictions. Curve C is the change in surface tension per area at 18 °C. Other parameters include χ_s = 1.0, Z_p = 852, $\varphi_p^b = 1.43 \times 10^{-3}$, $\bar{V}_p$ = 99.1 cm³/mol, and $\bar{V}_s$ = 94.0 cm³/mol.

the total free energy change, is quite different for the two cases.

This difference can be attributed to the redistribution of polymer between the interphase and bulk solution in the full equilibrium case. When the interphase is compressed to intermediate separations, additional polymer enters the interphase from bulk solution; the change in the adsorbed amount is positive as shown in Figure 4. The polymer volume fraction at the gap midpoint is therefore greater for full equilibrium (solid curves) than for constrained equilibrium (dashed curves). Consequently, the disjoining pressure is also greater for full equilibrium than

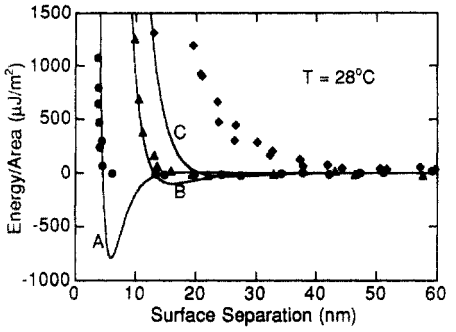

Figure 8. Experimental and calculated compression work per area for two interacting layers of PS adsorbed onto mica from CP at 28 °C. The experimental data (ref 30) are for PS molecular weights of 1.15×10^5 g/mol (circles, $Z_p = 200$), 5.15×10^5 g/mol (triangles, $Z_p = 895$), and 1.080×10^6 g/mol (diamonds, $Z_p = 1877$). Curves A–C are the corresponding model predictions. Other parameters include $\chi_s = 1.0$, $\chi = 0.460$, $\varphi_p^b = 1.43 \times 10^{-3}$, $\bar{V}_p = 99.1$ cm³/mol, and $\bar{V}_s = 94.0$ cm³/mol.

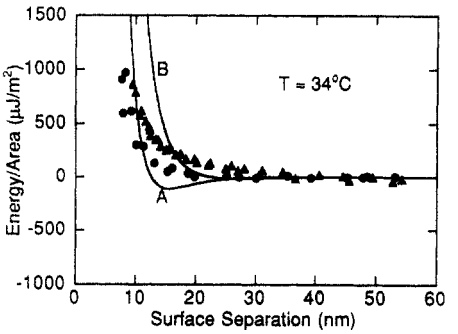

Figure 9. Experimental and calculated compression work per area for two interacting layers of PS adsorbed onto mica from CP at 34 °C. The experimental data (ref 30) are for PS molecular weights of 4.90×10^5 g/mol (circles, $Z_p = 852$) and 1.080×10^6 g/mol (triangles, $Z_p = 1877$). Curves A and B are the corresponding model predictions. Other parameters include $\chi_s = 1.0$, $\chi = 0.433$, $\varphi_p^b = 1.43 \times 10^{-3}$, $\bar{V}_p = 99.1$ cm³/mol, and $\bar{V}_s = 94.0$ cm³/mol.

for constrained equilibrium at intermediate separations. Further compression ejects polymer from the gap. When the polymer adsorbed amount falls to the large separation value, the full and constrained equilibrium cases have the same φ_{ads}, φ_p^m, π, and $\Delta\gamma$ (Figure 3). Upon further compression, the constrained equilibrium interphase contains more polymer than the full equilibrium interphase, so the disjoining pressure is more repulsive (Figure 4). The corresponding work of compression becomes more repulsive at a somewhat smaller separation (Figure 3).

Figure 5 shows the work of compression of a polymer interphase for several polymer chain lengths. For each curve, the gap half-width is scaled on the square root of the number of segments in the polymer chain for that case. The unscaled curves are shown in the inset. The depth of the attraction increases as the chain length decreases. Although one might expect attraction to increase with chain length because of enhanced bridging, the increase in the adsorbed amount with the square root of chain length[22] produces a greater increase in osmotic repulsion. The superposition of compression work for different chain lengths at small scaled separations agrees with the scaling observed in experimental data from the surface forces apparatus.[29,30]

We compare theoretical predictions for the work of compression with experimental data obtained from the surface forces apparatus in Figures 6–9. Hu and Granick[30] measured interaction forces for the compression of polystyrene (PS) layers adsorbed on mica surfaces from cyclopentane (CP). Procedures for establishing model parameters from experimental conditions were reviewed earlier and have been discussed in detail elsewhere.[22]

The physical properties of pure PS and CP lead to $\varphi_p^b = 0.953(\text{cm}^3/\text{g})c_p^b$ where c_p^b is the mass concentration of PS in bulk solution, $\bar{V}_p = 99.1$ cm³/mol, and $\bar{V}_s = 94.0$ cm³/mol. Schmidt and Burchard's correlation[31] gives the radius of gyration PS in many Theta solvents; from this, we calculate $l = 1.70$ nm and $Z_p = 1.73 \times 10^{-3}$ (mol/g)M_{PS} where M_{PS} is the PS molecular weight. Using the form of the Flory–Huggins equation of state given in the Appendix, we have determined the variation of χ with T by constructing a Shultz–Flory plot[32] from critical temperature data for PS–CP solutions,[33] yielding

$$\chi = \frac{1}{2} - 1.441\left(1 - \frac{292.8\ \text{K}}{T}\right)$$

The value of χ_s for this system is not known; we use $\chi_s = 1.0$ for most calculations.

As discussed by Patel and Tirrell,[29] Derjaguin integration[34] shows that the measured force F between the two curved mica surfaces equals $2\pi R$ times the interaction energy per area between two planar surfaces (R is the mean radius of curvature of the mica surfaces). The work per area ($2A_s$) given by eq 29 is multiplied by $2(2\pi)$ for comparison with experimental values of F/R. Dimensionless gap half-width times $2l$ produces the surface separation.

Theoretical predictions for the work per area for compression of 5.15×10^5 g/mol PS at 23 °C are compared with data from the surface forces apparatus[30] in Figure 6. This temperature is just above the Theta temperature of 19.6 °C. Curves A–D depict the compression work per area for $\chi_s = 0.25$, 0.50, 1.0, and 1.5, respectively. As $RT\chi_s$ becomes comparable to the thermal energy per mole RT, the compression work becomes independent of χ_s. Adjustment of χ_s would not improve the agreement between model predictions and experimental data, so we choose $\chi_s = 1.0$.

Curve E in Figure 6 shows the change in the surface tension upon compression of the interphase. Although this curve has the correct qualitative shape, the attractive minimum is too deep, and the separation at which strong repulsion is encountered is too small. Similar features are observed under other conditions. As was found for full equilibrium conditions, the differential of the surface tension given by eq 26 shows that the disjoining pressure (eq 28) equals the sum of an attractive contribution, the change in surface tension, plus an additional osmotic repulsion. Hence we expect the change in surface tension to be more attractive than the compression work.

Figure 7 depicts the compression work per area for 4.90×10^5 g/mol PS at 18 °C and 28 °C. The surface forces data[30] and the calculated work at 18 °C (poor solvent conditions) display attractive minima; much less attraction is seen in the data and calculated work at 28 °C (good solvent conditions). For both the experimental and calculated interactions, the ultimate repulsion occurs at a larger separation for the poor solvent. Curve C is the change in the surface tension at 18 °C.

Interactions for 1.15×10^5, 5.15×10^5, and 1.080×10^6 g/mol PS at 28 °C are shown in Figure 8. The calculated work per area agrees quantitatively with the surface forces data for the 1.15×10^5 and 5.15×10^5 molecular weights, although the predicted work in the former case displays an attractive minimum not seen in the data. The cause of this discrepancy is not clear. The calculated work per area for 1.080×10^6 g/mol PS has a substantially shorter range than the measured interaction. Although we can

only speculate as to the cause of this disagreement, Hu and Granick[30] observe that this set of data does not collapse onto a single curve with data at 28 °C for other PS molecular weights when the separation is scaled with the radius of gyration. The calculated curves A, B, and C scale in the same way (not shown) as the curves in Figure 5.

Figure 9 shows compression work per area for 4.90×10^5 and 1.080×10^6 g/mol PS at 34 °C. The calculated work displays slight attraction, but the surface forces data are purely repulsive. Also, the calculated interaction becomes strongly repulsive at separations larger than those observed experimentally. Nevertheless, the qualitative agreement between model predictions and experimental data is good.

V. Conclusions

A. Compression of Polymer Interphases. Conservation of energy and conservation of linear momentum must yield identical expressions for the work performed to achieve a specified deformation of a polymer interphase. As first pointed out by Evans and Needham,[21], work calculations based on the energy balance of Mackor and van der Waals,[5] eqs 1, 3, and 4, are not consistent with the stress and work obtained from a force balance. Evans resolves this inconsistency by deriving an expression for the compression work from a mechanical energy balance. For interactions of lipid bilayers mediated by nonadsorbing polymer in solution, the compression work calculated from the integral of the disjoining pressure is more repulsive and has a longer range than the interaction based on the change in the surface tension.[21] Similar results are seen in Figures 1, 3, 6, and 7 of this work for the compression of adsorbed polymer layers.

The reason for this difference becomes apparent when we consider the forms of work potentials that are appropriate for various forces which may act upon an interphase. Evans and Needham[21] discuss, as an example, the work potential associated with volumetric changes of a system due to changes in pressure. The differential work potential for this case is $-P\delta V$; it is certainly not the variation of the Gibbs potential $-\delta(PV)$. For finite volumetric changes at constant temperature and composition, the total work is the integral of the work potential, that is

$$W = -(P_2V_2 - P_1V_1) + \int_{P_1}^{P_2} V\,dP = -\int_{V_1}^{V_2} P\,dV \quad (43)$$

Calculating the work from the variation of the Gibbs potential would be incomplete: the integral of a $V\,dP$ term must be added to the change in the Gibbs potental to give the expected result.

Similar considerations apply to interphases for which γA_s is analogous to the Gibbs potential. The work potential for creating new interphase area is $\gamma\delta A_s$. However, the work potential for other changes within the interphase at constant area *is not* $A_s\delta\gamma$ as is clearly stated by Lyklema.[25] Equations 1, 3, and 4 are based on the premise that the work potential for compression of an interphase is the integral of $A_s\delta\gamma$. If the total work for compression of an interphase is to be calculated from the change in the surface tension, then a correction analogous to the $V\,dP$ term must be added to $A_s\delta\gamma$.

These considerations are borne out by a rigorous derivation of a free energy balance for compression of a polymer interphase. Application of conservation principles first provides a generic free energy balance that states, for a system at constant temperature undergoing reversible deformations, that the change of the free energy of the system equals the total stress times strain in the system, plus the net input of energy due to the addition of mass. Equation 18 provides this balance statement in variational form. Thus the variation of the Helmholtz free energy, equal to the total work potential, is the sum of the work potentials associated with an overall volumetric change, addition of mass, and deformation of the interphase.

We then consider the particular case of compression of an interphase contained between two parallel planar surfaces. For deformations which change the area of the interphase at constant surface separation, eqs 25 and 26 indicate that the appropriate work potential is $2\gamma A_s$ as expected. For deformations which compress the interphase at constant area, eqs 27 and 28 give the osmotic pressure difference as the appropriate work potential, as required by the conservation of linear momentum. We observe that the expressions for the surface tension of polymer interphases and the stresses arising from their compression are closely related to the corresponding expressions for interphases containing distributions of diffuse electrostatic charge.[12]

One notable conclusion is that for the compression of polymer interphases under full equilibrium conditions, the compression work is monotonically repulsive, in contrast with the monotonic attraction found by de Gennes.[8] As the interphase is compressed, the "chemical" part of the disjoining pressure becomes more negative as the chains that remain in the interphase participate in more polymer–surface contacts. However, the repulsive osmotic stress caused the increasing polymer concentration in the interphase outweighs the attraction at all separations.

B. Comparisons of Theory and Experiment. Satisfactory agreement between SCF model predictions and measured polymeric interactions has been achieved without arbitrary adjustment of any model parameters. All model parameters come from given experimental conditions, component physical properties, and data from selected polymer solution experiments. For the comparisons of theoretical and experimental interactions in Figures 6–9, the level of quantitative agreement varies. We see excellent agreement for lower PS molecular weights at 28 °C (Figure 8), satisfactory agreement for similar PS molecular weights at lower temperatures (Figures 6 and 7), and relatively poor agreement for the highest PS molecular weight at 28 °C (Figure 8). At 34 °C, the predicted and measured interactions are of similar magnitude, but the shapes of the repulsions differ.

Preliminary comparisons of calculated and measured compression work data for interactions of PS layers adsorbed onto mica from cyclohexane[29] indicate that the present model gives satisfactory predictions of the location of the strong repulsion at small separations. The depth of the attraction for interactions in poor solvents is not predicted accurately, though. These results will be detailed in a subsequent publication.

Three main issues must be considered as we compare SCF model predictions and data for real polymer interphases. First, we have used a variant of the Flory–Huggins equation of state to describe polymer–solvent interactions. More realistic equations, such as the compressible lattice fluid equation of state,[35] may allow more accurate predictions, especially at temperatures away from the theta point. Compressibility effects, recently incorporated into a SCF lattice model for grafted polymer layers,[36] seem to be significant for interphase structure. The relevance of these issues can be explored through further model development.

Second, our regular perturbation solution of the general SCF equations has not been carried beyond the first term, thereby precluding end effects or "tails". The truncation of the perturbation expansion is equivalent to the ground-state solution developed previously.[11] This approximation will lead to errors in the predicted forces at ranges comparable to the polymer's root-mean-squared end-to-end distance. Presumably the present model would predict greater repulsion that might be measured experimentally due to the absence of attractive bridging configurations formed from tails. Since tails make a minor contribution to the total adsorbed mass of polymer for the experimental conditions reviewed here,[40] we speculate that the bridging attraction due specifically to tails will not be significant at separations less than the polymer's root-mean-squared end-to-end distance. However, the relative contribution at greater separations could be important. This point can be resolved through a more complete model which includes more terms in the perturbation solution.

Finally, like earlier models, the present model cannot address equilibration issues which go beyond the question of interphase–solution exchange. The time scale for rearrangement of polymer molecules within a deforming interphase may be much longer than practical experimental time scales. Internal equilibration is a primary issue in most surface forces measurements involving polymers,[29] including those featured[30] in Figures 6–9. Deeper understanding of this issue will likely require new approaches to interphase modeling based on nonequilibrium statistical mechanics or dynamic simulation, not to mention further experimentation.

Acknowledgment. I thank S. Granick and H. W. Hu for providing surface forces data, and W. B. Russel for his comments and discussion. This work was supported by Engineering Excellence funds from the Texas Engineering Experiment Station at Texas A&M University, by the National Science Foundation through Grants CTS 9009754 and CTS-9258137, and by funds from the Shell Development Co.

Appendix

Extended Flory–Huggins Equation of State. Helfand and Sapse[37] introduced an extended form of the Flory–Huggins equation of state which explicitly accounts for volume differences between solvent molecules and polymer segments. The free energy density, given by

$$a_h = \rho_p\mu_p^\circ + \rho_s\mu_s^\circ - P^\circ + \rho_s \ln(\varphi_s) + \frac{\rho_p}{Z_p}\ln(\varphi_p) + \chi\rho_s\varphi_p \quad \text{(A1)}$$

is actually a mixing free energy for creating a homogeneous polymer–solvent mixture from pure components at reference conditions (superscript o). The usual definitions of the partial molar free energies give

$$\mu_p \equiv \left(\frac{\partial a_h}{\partial \rho_p}\right)_{T,\rho_s} = \mu_p^\circ + \frac{1}{Z_p}\ln(\varphi_p) + \left(\frac{1}{Z_p} - \frac{\bar{V}_p}{V_s}\right)\varphi_s + \chi\frac{\bar{V}_p}{\bar{V}_s}\varphi_s^2 \quad \text{(A2)}$$

$$\mu_s \equiv \left(\frac{\partial a_h}{\partial \rho_s}\right)_{T,\rho_p} = \mu_s^\circ + \ln(\varphi_s) + \left(1 - \frac{\bar{V}_s}{\bar{V}_p Z_p}\right)\varphi_p + \chi\varphi_p^2$$

which reduce to the usual forms for equal molar volumes. The mixing free energy defined in eq 41 is found to be

$$\bar{V}_p\Delta a = \frac{\varphi_p}{Z_p}\ln\left(\frac{\varphi_p}{\varphi_p^b}\right) + \frac{\bar{V}_p}{\bar{V}_s}\left[\varphi_s\ln\left(\frac{\varphi_s}{\varphi_s^b}\right) + \left(1 - \frac{\bar{V}_s}{\bar{V}_p Z_p}\right)(\varphi_p - \varphi_p^b) - \chi(\varphi_p - \varphi_p^b)^2\right] \quad \text{(A3)}$$

which is similar in form to expressions arising in the lattice model of Scheutjens and Fleer.[7,10]

References and Notes

(1) Derjaguin, B. V.; Landau, L. *Acta Phys. Chim USSR* **1941**, *14*, 633.
(2) Verwey, E. J. W.; Overbeek, J. Th. G. *Theory of the Stability of Lyophobic Colloids*; Elsevier: Amsterdam, 1948.
(3) Ploehn, H. J.; Russel, W. B. *Adv. Chem. Eng.* **1990**, *15*, 137.
(4) Halperin, A.; Tirrell, M.; Lodge, T. P. *Adv. Polym. Sci.* **1991**, *100*, 31.
(5) Mackor, E. L. *J. Colloid Sci.* **1951**, *6*, 492. Mackor, E. L.; van der Waals, J. H. *J. Colloid Sci.* **1952**, *7*, 535.
(6) Ash, S. G.; Everett, D. H.; Radke, C. J. *J. Chem. Soc., Faraday Trans. 2* **1973**, *69*, 1256.
(7) Scheutjens, J. M. H. M.; Fleer, G. J. *J. Phys. Chem.* **1979**, *83*, 1619. Scheutjens, J. M. H. M.; Fleer, G. J. *J. Phys. Chem.* **1980**, *84*, 178.
(8) de Gennes, P. G. *Macromolecules* **1982**, *15*, 492.
(9) Klein, J.; Pincus, P. *Macromolecules* **1982**, *15*, 1129.
(10) Scheutjens, J. M. H. M.; Fleer, G. *Macromolecules* **1985**, *18*, 1882. Fleer, G. J.; Scheutjens, J. M. H. M. *J. Colloid Interface Sci.* **1986**, *111*, 504.
(11) Ploehn, H. J. Ph.D. Dissertation, Princeton University, 1988.
(12) Rossi, G.; Pincus, P. *Europhys. Lett.* **1988**, *5*, 641. Rossi, G.; Pincus, P. *Macromolecules* **1989**, *22*, 276.
(13) Ingersent, K.; Klein, J.; Pincus, P. *Macromolecules* **1990**, *23*, 548.
(14) Slattery, J. C. *Interfacial Transport Phenomena*; Springer-Verlag: New York, 1990.
(15) Edwards, D. A.; Brenner, H.; Wasan, D. T. *Interfacial Transport Processes and Rheology*; Butterworth-Heinemann: Boston, MA, 1991.
(16) Prager, W. *Introduction to the Mechanics of Continua*; Dover: New York, 1961.
(17) Schowalter, W. R. *Mechanics of Non-Newtonian Fluids*; Pergamon: Oxford, U.K., 1978.
(18) Slattery, J. C. *Momentum, Energy, and Mass Transfer in Continua*, 2nd ed.; Robert E. Krieger: Huntington, NY, 1981.
(19) Helfand, E. *J. Chem. Phys.* **1975**, *62*, 999.
(20) Hong, K. M.; Noolandi, J. *Macromolecules* **1981**, *14*, 727.
(21) Evans, E.; Needham, D. *Macromolecules* **1988**, *21*, 1823. Evans, E. *Macromolecules* **1989**, *22*, 2277.
(22) Ploehn, H. J. *Macromolecules*, preceding paper in this issue.
(23) Kirkwood, J. G.; Buff, F. P. *J. Chem. Phys.* **1949**, *17*, 338.
(24) Everett, D. H. *Pure Appl. Chem.* **1972**, *31*, 579.
(25) Lyklema, J. *Fundamentals of Interface and Colloid Science, Volume I: Fundamentals*; Academic: London, 1991.
(26) Edwards, S. F. *Proc. R. Soc. London* **1965**, *85*, 613. de Gennes, P. G. *Scaling Concepts in Polymer Physics*; Cornell University: Ithaca, NY, 1985. de Gennes, P. G. *Adv. Colloid Interface Sci.* **1987**, *27*, 189.
(27) van der Beek, G. P. Ph.D. Dissertation, Wageningen Agricultural University, 1991.
(28) Brandup, J.; Immergut, E. H. *Polymer Handbook*; Wiley: New York, 1982.
(29) Patel, S. S.; Tirrell, M. *Annu. Rev. Phys. Chem.* **1989**, *40*, 597.
(30) Hu, H.-W.; Granick, S. *Macromolecules* **1990**, *23*, 613.
(31) Schmidt, M.; Burchard, W. *Macromolecules* **1981**, *14*, 210.
(32) Schultz, A. R.; Flory, P. J. *J. Am. Chem. Soc.* **1952**, *74*, 4760.
(33) Saeki, S.; Kuwahara, N.; Konno, S.; Kaneko, M. *Macromolecules* **1973**, *6*, 589.
(34) Derjaguin, B. V. *Kolloid. Zh.* **1934**, *69*, 155.
(35) Sanchez, I. C.; Lacombe, R. H. *Macromolecules* **1978**, *11*, 1145.
(36) Peck, D. G.; Johnston, K. P. *Macromolecules* **1993**, *26*, 1537.
(37) Helfand, E.; Sapse, A. M. *J. Polym. Sci., Polym. Symp.* **1976**, *54*, 289.
(38) Davis, H. T.; Scriven, L. E. *Adv. Chem. Phys.* **1982**, *49*, 357.
(39) Anderson, J. L. *Adv. Colloid Interface. Sci.* **1982**, *16*, 391. Adamski, R. P.; Anderson, J. L. *Biophys. J.* **1983**, *44*, 79.
(40) Scheutjens, J. M. H. M.; Fleer, G. J.; Cohen Stuart, M. A. *Colloids Surf.* **1986**, *21*, 285.